Insight into the mechanism behind oral bioavailability-enhancement by nanosuspensions through combined dissolution/permeation studies☆

Jakob Tobias Lynnerup [a,b], Jonas Borregaard Eriksen [a], Annette Bauer-Brandl [a], Ann Mari Holsæter [b], Martin Brandl [a,*]

[a] Department of Physics Chemistry and Pharmacy, University of Southern Denmark, Odense M, Denmark
[b] Drug Transport and Delivery Research Group, Department of Pharmacy, Faculty of Health Sciences, University of Tromsø The Arctic University of Norway, Tromsø 9037, Norway

ARTICLE INFO

ABSTRACT

As numerous new drug candidates are poorly water soluble, enabling formulations are needed to increase their bioavailability for oral administration. Nanoparticles are a conceptually simple, yet resource consuming strategy for increasing drug dissolution rate, as predicting in vivo oral absorption using in vitro dissolution remains difficult. The objective of this study was to obtain insight into nanoparticle characteristics and performance utilizing an in vitro combined dissolution/permeation setup. Two examples of poorly soluble drugs were examined (cinnarizine and fenofibrate). Nanosuspensions were produced by top-down wet bead milling using dual asymmetric centrifugation, obtaining particle diameters of approx. 300 nm. DSC and XRPD studies indicated that nanocrystals of both drugs were present with retained crystallinity, however with some disturbances. Equilibrium solubility studies showed no significant increase in drug solubility over the nanoparticles, as compared to the raw APIs. Combined dissolution/permeation experiments revealed significantly increased dissolution rates for both compounds compared to the raw APIs. However, there were substantial differences between the dissolution curves of the nanoparticles as fenofibrate exhibited supersaturation followed by precipitation, whereas cinnarizine did not exhibit any supersaturation, but instead a shift towards faster dissolution rate. Permeation rates were found significantly increased for both nanosuspensions when compared to the raw APIs, indicating a direct implication that formulation strategies are needed, be it stabilization of supersaturation by precipitation inhibition and/or dissolution rate enhancement. This study indicates that in vitro dissolution/permeation studies can be employed to better understand the oral absorption enhancement of nanocrystal formulations.

1. Introduction

Most drug candidates in the pharmaceutical pipelines are poorly water soluble. This poses a potential problem of poor oral bioavailability as the active pharmaceutical ingredient (API) must dissolve to be absorbable in the gastrointestinal tract. Poorly soluble drugs need formulations that enhance the solubility to obtain sufficient bioavailability after oral administration (Bergstrom et al., 2016; Buckley et al., 2013; Keseru and Makara, 2009). One approach to increase the oral absorption of poorly soluble drugs is to reduce the size of the drug particles.

According to the Nernst-Brunner equation, the dissolution rate of particles increases by size reduction due to a higher specific surface area (Nernst, 1904). During dissolution, it is also observed that small particles may exceed the equilibrium solubility, although this may still be discussed as being a matter of experimental methods used (Bauer-Brandl and Brandl, 2020). From various studies in literature, it is known that nano-milled fenofibrate yields faster dissolution, which upon oral administration results in earlier t_{max}, higher C_{max} and larger AUC as compared to fenofibrate of larger crystal size, and decent IVIVC indicates that oral bioavailability of fenofibrate is dissolution rate-limited

☆ All authors have read and agreed to the submitted manuscript.
* Corresponding author.
E-mail address: mmb@sdu.dk (M. Brandl).

(Wang et al., 2012; Xu et al., 2014). While dissolution rate enhancement through nano-milling is reported in literature (van Eerdenbrugh et al., 2008), only few data on its correlation with enhanced bioavailability are available. Mishra and colleagues (Mishra et al., 2016) report earlier t_{max}, higher C_{max} and larger AUC for orally administered (rats) nanomilled cinnarizine as compared to reference.

With recent advancements concerning milling processes in the pharmaceutical industry, it is now possible to produce nanoparticles down to the 100–200 nm range. Rapamune® (Sirolimus, Wyeth), EMAND® (Aprepitant, Merck), and TriCor® (Fenofibrate, Abbott) are examples of marketed products prepared by ball milling of aqueous suspensions of the APIs containing surfactants and polymers, stabilizing the comminuted particles, and preventing their re-agglomeration (Kesisoglou et al., 2007). If the nanoparticles are not sufficiently stabilized, a risk of agglomeration persists, as well as crystal growth due to Ostwald ripening, or chemical degradation e.g., by hydrolysis during storage. Therefore, it should be considered to incorporate the nanosuspensions in solid dosage forms, which can be achieved by techniques such as spray- or freeze-drying and layering of pellets for multiple-unit pellet systems (Schmidt and Bodmeier, 1999; Van Eerdenbrugh et al., 2008).

Finding the optimum composition of surfactants and polymers for a certain API often requires screening of numerous compositions/ratios of the respective components (Van Eerdenbrugh et al., 2009). This process is usually very time-consuming as most planetary ball mills must mill for hours and can only mill a small number of formulations at a time. As wet bead milling is one of the most utilized nanocrystal production techniques, there is a need for screening upscaling from laboratory to production (Tuomela et al., 2015). In a recent study, Hagedorn et al. (2017) applied dual centrifugation to prepare nanosuspensions. The technique applies very high power to zirconium beads in small, closed containers, resulting in homogenous nanoparticles forming rapidly, allowing screening of multiple formulations simultaneously (Hagedorn et al., 2017). A good comparability between nanoparticle formulations processed by dual centrifugation and different sized agitator bead mills were also shown. Identical nanoparticles were obtained from dual centrifugation and small-scale agitator milling in relation to solid-state, particle size, and size distribution. However, limitations of lower specific grinding energy using large-scale agitator milling resulted in larger particles when compared to dual centrifugation (Hagedorn et al., 2019).

Dual asymmetric centrifugation enables fast mixing or grinding of materials by rotating the sample holder in two directions simultaneously: a primary rotation around the base and a secondary rotation of the sample holder in the opposite direction (Fig. 1). This leads to a very frequent and rapid sample movement. Furthermore, adding milling- or homogenization aids in the form of heavy beads (i.e., zirconia oxide beads) to the sample increases the efficiency of the milling process. The dual asymmetric centrifuge "SpeedMixer™" used in this study has previously been utilized to prepare liposomes for different medical purposes (Holsæter et al., 2022; Ingebrigtsen et al., 2017a, 2017b; Massing et al., 2008). This technique is also often referred to as "dual centrifugation", but not all dual centrifuges have the asymmetric construction as is the case for the SpeedMixer™, and thus "dual asymmetric centrifugation" gives a more detailed description as the dual rotor is asymmetrically built and it carries only one rotating unit (Fig. 1) (Massing et al., 2017). To allow small sample volumes (2 mL Twist-top vials) and multiple samples to be prepared simultaneously, an in-house 3D-printed sample adapter was applied (Fig. 1).

Hagedorn et al. (2017) analyzed the performance of milling processes with respect to particle size distribution, its stability, and morphology. In terms of performance, the dissolution kinetics of the nanosuspensions upon dilution is a key parameter. It has previously been claimed by Juenemann et al. (2011), that nanofiltration using filters with pore sizes of 100 nm and below provides useful dissolution profiles of nanoparticle formulations with respect to absorption. Using different sizes of filters, they revealed different dissolution profiles in biorelevant media, where the ones measured using small pore sizes gave the best correlation to in vivo behavior (Juenemann et al., 2011).

Despite the vast number of recent studies on nano-milling of poorly soluble drugs, the selection of optimum process parameters and formulation additives for nano-formulations in order to achieve the desired oral absorption enhancement is still challenging and predictions based on in vitro parameters like particle size, solubility and dissolution rate still may be erroneous (Singhal et al., 2022). Examination of not only dissolution and solubility properties of different nanoparticle formulations, but also the permeation rate in biomimetic setups are important parameters of pre-formulation for oral absorption. Furthermore, over the past couple of decades, the combined dissolution/permeation experiments have increased in popularity to predict the in-vivo performance ranking between enabling formulations of poorly soluble drugs (Kataoka et al., 2003; Vinarov et al., 2021). The permeation allows to differentiate freely molecularly dissolved species, that are able to permeate, from solubilized species, such as micelles, cyclodextrins, etc., that do not permeate but would slip through the filters (Buckley et al., 2013). The combination of dissolution and permeation in addition reveals the kinetic interplay of the two processes. Studies have shown that permeation out of a dissolution vessel to an "absorptive sink" may extend the period of supersaturation and thus a more substantial parachute effect can be observed as compared to classical dissolution experiments in closed systems (Bevernage et al., 2012; Sironi et al., 2017). Inclusion of an absorptive sink in combined dissolution/permeation setups is thus regarded to be more biopredictive. A setup similar to the one used here has been demonstrated to detect supersaturation from a commercial nanocrystalline fenofibrate product, an observation not made earlier with conventional dissolution experiments (Sironi et al., 2017). It is not known, however, whether

Fig. 1. Inside of the SpeedMixer™ type "DAC 150.1 FVZ-K" (left), sample adapter for 6 Twist-Top vials (middle), and schematic representation of rotation pattern (right).

such supersaturation would be observed with all nano-milled drugs under absorptive sink conditions.

In this study, nanosuspensions of the poorly soluble model compounds fenofibrate and cinnarizine were prepared via dual asymmetric centrifugation, and the performance of the products was measured with dissolution/permeation experiments on a reversed-Franz cell setup. The aim was to investigate whether dissolution/permeation experiments can give additional insight into the performance and characteristics of poorly soluble drugs during nanomilling, beyond the traditional particle size and dissolution rate analysis.

2. Materials and methods

2.1. Chemicals

Fenofibrate, cinnarizine, sodium phosphate monobasic dihydrate, sodium phosphate dibasic dihydrate, and trifluoroacetic acid were purchased from Sigma Aldrich (Brøndby, Denmark). Hydroxypropyl methylcellulose TC-5 E (HPMC) of pH. Eur. quality was donated as a gift from JRS Pharma GmbH & Co. KG (Rosenberg, Germany). Sodium dodecyl sulfate (SDS) was purchased from Caesar & Loretz GmbH (Hilden, Germany). 2-hydroxypropyl-β-cyclodextrin (HP-β-CD) was bought from Abcr GmbH (Karlsruhe, Germany). Acetonitrile of HPLC quality was purchased from VWR international A/S (Søborg, Denmark). The water used in experiments was highly purified, prepared by a Milli-Q reference $A+$ water purification system from Merck KGaA (Darmstadt, Germany). If not otherwise stated, the chemicals were of analytical grade.

2.2. Media preparation

30 mM phosphate buffer was prepared by dissolving 11 mM sodium phosphate dibasic dihydrate and 19 mM sodium phosphate monobasic dihydrate in highly purified water. The pH was adjusted to 6.5 with 1 M sodium hydroxide solution or 1 M hydrochloric acid solution.

2.3. Quantification of fenofibrate and cinnarizine

Cinnarizine and fenofibrate were quantified via high-performance liquid chromatography-ultraviolet (HPLC-UV). Details for the detection of each compound are stated in table 1.

2.4. Nano-milling of API suspensions via dual-asymmetric centrifugation

The composition of polymers and surfactants used in the suspensions for nano-milling of fenofibrate and cinnarizine was the most optimal composition earlier found for fenofibrate (Hagedorn et al., 2017; Knieke et al., 2013). In brief, 1000 mg of water containing 2% (m/V) HPMC and

Table 1
HPLC conditions used for quantification of fenofibrate and cinnarizine.

Compound	Fenofibrate	Cinnarizine
Apparatus	2690 HPLC apparatus with a 996-photodiode array detector from Waters Corporation (Milford, MA, USA)	2695D HPLC apparatus with a 2487 dual λ absorbance detector from Waters Corporation.
Column	XSelect CSH C18 column from Waters Corporation.	Dionex™ reversed-phase C18 LC-column from Thermo Fischer Scientific Inc. (Roskilde, Denmark) (product number: 059,133)
Temperature	40 °C	40 °C
Flowrate	1 mL/min	1 mL/min
Mobile phase	80% acetonitrile, 19.98% water and 0.02% trifluoroacetic acid	60% acetonitrile, 39.96% water and 0.04% trifluoroacetic acid
Retention time	1.6 min	2.6 min

0.075% (m/V) SDS, 1000 mg YTZ® zirconia oxide beads from Nikkato corporation (Sakai, Japan), and 100 mg of fenofibrate or cinnarizine was weighed into a 2 mL Twist-top vial.

The nanosuspensions were prepared using a SpeedMixer™ dual asymmetric centrifuge 150.1 FVZ-K from Synergy Devices Ltd. (High Wycombe, United Kingdom). If not otherwise stated, the twist-top vials with drug suspensions were milled for 90 min at 1500 rpm. After milling, the nanosuspensions were centrifuged on a bench-top centrifuge (Microfuge 20R from Beckmann Coulter Inc., Indianapolis, IN, USA) at 1000x G for 5 min. The supernatant was collected into a new twist-top vial.

Heat production from the dual asymmetric centrifugation was limited by milling in cycles of 5 min (supplementary information). Between each cycle, the sample adaptor was stored inside a refrigerator for 2 min or until the samples were cooled to room temperature, before the milling was resumed.

2.5. Particle size measurements with dynamic light scattering

The particle size distribution was measured using dynamic light scattering on a ZetaSizer Nano ZS from Malvern Panalytical Ltd. (Malvern, United Kingdom). 3 μL nanosuspension was diluted in 1000 μL of highly purified water saturated with the studied drug compound in disposable plastic cuvettes. Particles in the size range from 0.3 nm to 10 μm were measured in three runs of 60 s at 25 °C with a refractive index at 1.33 and a dielectric constant at 78.6. The mean particle size is reported as z-average and polydispersity index (PDI) that the Malware apparatus software calculated.

2.6. Differential scanning calorimetry

The melting points for raw products and nanoparticles of fenofibrate and cinnarizine were measured by differential scanning calorimetry (DSC) using a DSC 8500 from PerkinElmer Inc. (Waltham, MA, USA). The nanocrystals were obtained by air-drying the supernatant from the nanosuspensions on a piece of aluminum foil overnight. Around 2 mg of fenofibrate or 4 mg of cinnarizine or their respective nanocrystals were sealed in 50 μL aluminum pans. The measurements were performed from 25 to 150 °C with an increase in temperature of 3 °C/min for fenofibrate and 10 °C/min for cinnarizine. The instrument was purged using nitrogen gas with a 20 mL/min flowrate.

2.7. X-ray powder diffraction

X-ray powder diffraction (XRPD) compared the crystal state of raw fenofibrate and cinnarizine with the produced nanoparticles using a MiniFlex 600 from Rigaku Corp. (Tokyo, Japan). The nanocrystals were obtained by drying the supernatant of the nanosuspensions on aluminum foil overnight and grinding the obtained aggregates to a fine powder with a mortar and pestle. Measurements were performed with Cu radiation, 20 kV, and 400 mA voltage. The samples were measured at a diffraction angle (2θ) varying from 5 to 45° with a sampling width of 0.02° at a scanning speed of 5 °/min.

2.8. Solubility measurements

The solubility of raw materials and nanoparticles were examined in phosphate buffer (composition given in Section 2.2), and relevant acceptor media compositions used in the dissolution/permeation experiments. Excess amounts of the raw material or 200 μL of the supernatant from the nanosuspensions were suspended in 10 mL phosphate buffer in amber flasks. Excess amounts of the raw compounds were also suspended in 10 mL of acceptor media 2% SDS and 5% HP-β-CD. The flasks were capped and placed in a shaking SW22 water bath from Julabo GmbH (Seelbach, Germany) set to 37 °C and 60 rpm. Samples of 500 μL were taken after 72 h and filtered using a 0.10 μm Whatman™

Anotop™ 10 inorganic membrane syringe filter from GE Healthcare (Little Chalfont, United Kingdom). The first 400 μL of the filtrate was discarded, and the remaining 100 μL samples were diluted in acetonitrile for quantification with HPLC-UV.

2.9. Combined dissolution/permeation experiments

Dissolution/permeation experiments were carried out using reversed Franz cell set-ups (PermeGear Inc., Hellertown, PA, USA), where the 1 mL compartment at the top served as acceptor and either a 5 mL (0.66 cm^2 permeation area) or 8 mL (1.0 cm^2 permeation area) compartment in the bottom as donor. In the bottom of the donor compartments, a small stirring bar was rotating at 500 rpm. The compartments were separated by a cellophane membrane, placed for 30 min in purified water, and then flushed in fresh purified water before use. A circulating water system was attached to the Franz cell to keep the temperature constant at 37 °C.

The acceptor compartments were filled with the most suitable acceptor media derived from a screening experiment (supplementary information), 2% SDS for fenofibrate and for cinnarizine 5% 2-hydroxypropyl-β-cyclodextrin. In the donor compartments, either 10 mg raw material or 100 μL nanosuspension (equal to 10 mg) was suspended in the phosphate buffer at the start of the experiments.

Dissolution samples of 500 μL, taken after 5, 15, 30, 60, 90, 120, 150, 180, 210, and 240 min from the bottom compartment, were filtered with a 0.10 μm pore-size Whatman™ Anotop™ 10 inorganic membrane filter. The first 300 μL were discarded, and the remaining 200 μL dissolution samples were immediately diluted with acetonitrile. Permeation samples of 500 μL were taken from the top chamber after 30, 60, 90, 120, 150, 180, 210, and 240 min and immediately diluted with acetonitrile. After sampling, the volume removed was replaced with phosphate buffer in the donor chamber and acceptor medium in the acceptor chamber.

2.10. Data analysis

The cumulative mass of permeated API was calculated according to Eq. (1),

$$m = \text{dil. factor} \cdot c \cdot V_{acceptor} + \sum_{n-1}^{0} \left(V_{sample} \cdot \text{dil. factor} \cdot c \right) \tag{1}$$

Where *m* is the cumulative mass, *c* is the concentration, and *V* is the volume.

2.11. Statistics

The lowest amount of API that was able to be detected, limit of detection (LOD), and quantified, limit of quantification (LOQ), based on the produced calibration curves were calculated according to Eq. (2) and Eq. (3) respectively,

$$LOD = \frac{3.3 \cdot SD}{S} \tag{2}$$

$$LOQ = \frac{10 \cdot SD}{S} \tag{3}$$

Where *S* is the slope of the regression and *SD* is the standard deviation of the y-intercept from the calibration curve.

A two-tailed Student's *t*-test was employed for the comparison of data sets, where a value of $p \leq 0.05$ was considered as significantly different.

3. Results and discussion

3.1. Particle size reduction of fenofibrate and cinnarizine via dual asymmetric centrifugation

The nanosuspensions prepared by dual asymmetric centrifugation appeared visually milky and homogenous. Analysis of the drug content in the supernatant upon bench top centrifugation indicated that not all the drug was finely dispersed, due to larger particles ending up in the pellet (supplementary information). Measurements of the particle size in the nanosuspensions by DLS showed that fenofibrate and cinnarizine particle sizes decreased when processed on the dual asymmetric centrifuge, initially rather rapidly then more and more slowly, when the process was followed over three hours (Fig. 2). The mean particle diameter of fenofibrate decreased from 573 nm to 259 nm during three hours of milling, and cinnarizine mean particle diameter decreased from 711 nm to 275 nm (time points 5 to 180 min in Fig. 2). Since the mean diameters of fenofibrate and cinnarizine were already down to 305 nm and 310 nm, respectively, after 90 min, we considered this to be the optimum milling conditions in further experiments. The PDI of fenofibrate stayed at approx. 0.20 during the entire milling period, indicating a narrow size distribution throughout the experiment. This indicates the stabilizer composition provides a stable suspension of fenofibrate, in accordance with previous studies (Hagedorn et al., 2017; Knieke et al., 2013). The PDI of cinnarizine decreased from 0.44 at 5 min to 0.25 after 150 min of milling, showing that the size distribution became more homogeneous over time. This indicates that larger particles or stronger agglomerates were present in the beginning. The re-increase from 0.25 to 0.29 from 150 to 180 min may indicate that a prolonged milling time might induce aggregation of cinnarizine because the chosen stabilizers are not efficient enough for the application of energy at the chosen
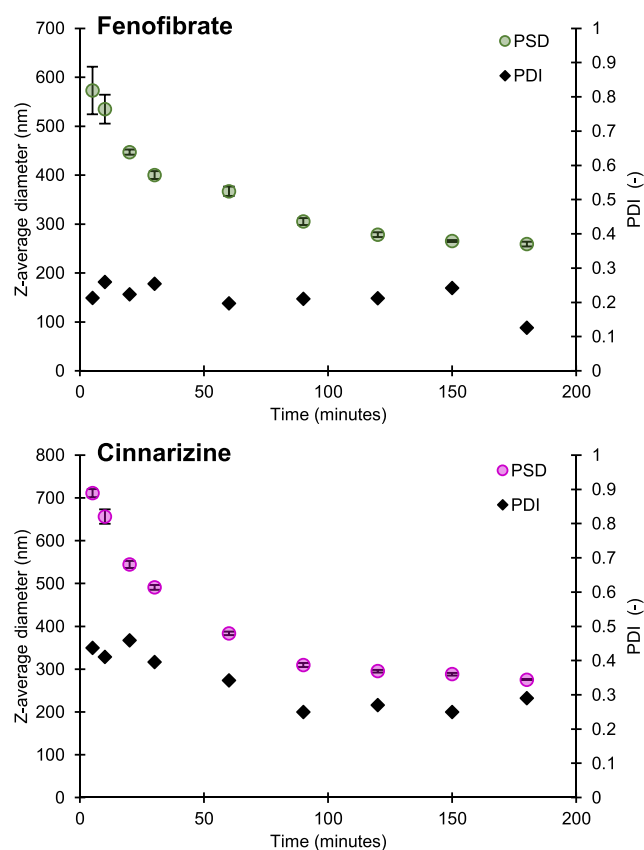

Fig. 2. Particle size distribution of fenofibrate (top) and cinnarizine (bottom) as the z-average diameter (circles), reported as mean ± SD (*n* = 3), and PDI (diamonds) from dynamic light scattering as a function of milling time.

rotational speed. Ripening caused by continuous milling using a planetary ball mill has also previously been shown for cinnarizine using a closely related stabilizer composition consisting of HPMC and dioctyl sulfosuccinate sodium salt (Bitterlich et al., 2014).

The mean particle sizes finally reached and kinetics of fenofibrate size-reduction were comparable to the results obtained by Hagedorn et al. (2017) by using the same stabilizer composition and drug load in twist-top vials. This indicates a similar process of deagglomeration and attrition, although, slightly larger particles were obtained after 90 min of dual asymmetric centrifugation. Despite very similar experimental conditions between our study and the study by Hagedorn et al. (2017), some differences are worth mentioning that can potentially affect the obtained nanoparticles. The dual centrifugation device used by Hagedorn et al. (2017) can actively cool samples, allowing for continuous milling at constant temperature (Hagedorn et al., 2017). Not only does the "stop-and-go" approach at room temperature employed in the current study take significantly longer, but also higher sample temperatures were reached (supplementary information). This might induce solid-state changes and could affect the smallest obtainable particle sizes. Slightly smaller zirconia beads of 0.1–0.2 mm diameter were used by Hagedorn et al. (2017) as compared to this study (0.3 mm) and can also be a factor for the larger particles obtained during this study.

Process parameters that influence final product properties during nanomilling are not only bead size and drug content, but also specific energy input, typically assigned by rpm, but dependent on geometry to produce different g values. These parameters are interdependent, e.g., decreasing grinding media diameter (i.e., bead size) and increasing energy input produces smaller particles (Ghosh et al., 2012; Willmann et al., 2022). Despite differences between the devices used in this study and by Hagedorn et al. (2017), both reach approx. the same maximum acceleration (Massing et al., 2017). However, only small differences between the setups might result in varying obtained nanoparticles.

3.2. Solid-state determination of nanoparticles

The nanoparticles produced by nanomilling of both fenofibrate and cinnarizine were examined for changes in their crystal state compared to the respective raw APIs, both by differential scanning calorimetry DSC and diffraction patterns measured by XRPD (Fig. 3).

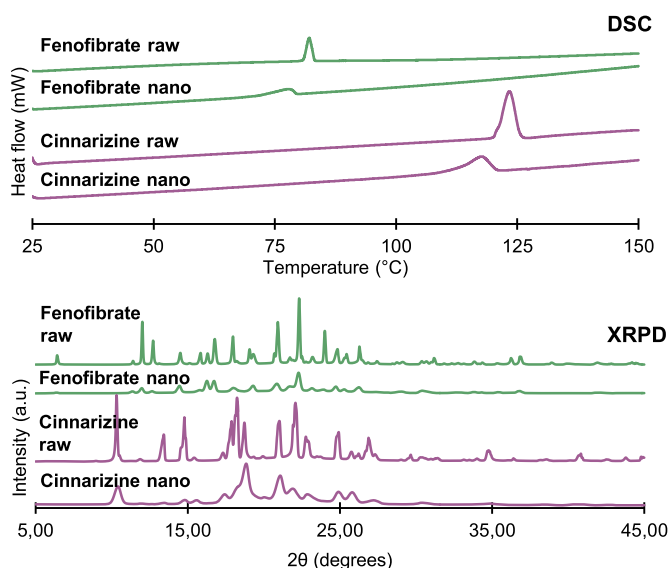All DSC patterns reveal a single exothermic peak, however,

Fig. 3. Typical DSC patterns (top) and XRPD diffractograms (bottom) of fenofibrate and cinnarizine and their respective nanoparticles produced by dual asymmetric centrifugation.

differences between the raw compounds and their respective nanoparticles were seen. Both nanoparticles of fenofibrate and cinnarizine showed less intensive and broader peaks with onsets at lower temperatures than the raw APIs. It is known that high-energy milling can affect the solid-state by inducing partly drug amorphization through interactions with stabilizers, resulting in melting point depression (Kumar and Burgess, 2014). It is also expected that small particles lower the melting point as it is dependent on particle diameter and curvature, thereby increasing the interface (Colombo et al., 2009). The DSC curves of the nanomilled drugs in Fig. 3 show a characteristic melting peak indicating that crystals are still present, yet with a lower onset temperature of melting and broader peaks, both of which could be caused by the smaller particle size, as the nanoparticles have a larger interface and possibly better contact to the aluminum pans as compared to the bulk. The absence of additional (exothermic) peaks indicates that there is no re-crystallization detectable (within the sensitivity of the applied method).

Also, in XRPD diffractograms, small particle sizes can cause peak broadening and halo effect due to the loss of long-range crystalline order by formation of partly disordered nanocrystals. Such solids are not completely transitioned to an amorphous form (Deng et al., 2008). The XRPD patterns of fenofibrate, cinnarizine, and their respective nanoparticles are comparable, yet with a decrease in peak intensity and slightly broader signals. Compared to the raw compounds, some peaks are not easily identifiable due to the broader and less intensive signals, as they overlap partly, and the reduction in peak intensity is not necessarily proportional between signals. Despite this, many identifiable peaks are visible, which indicates that the same crystalline phase of the compounds is present.

Combined results from DSC and XRPD support the hypothesis that nanocrystals are present. The chosen analytical approaches, however, cannot rule out a minor degree of amorphization or loss of crystalline order, caused by the extended application of energy during the milling process.

3.3. Equilibrium solubility measurements

The equilibrium solubilities of raw fenofibrate and cinnarizine and their nanoparticles were examined at 37 °C after 72 h of equilibration time to evaluate if the nanoparticles yield different equilibrium solubilities, results are listed in Table 2. No major increase in equilibrium solubility was observed neither for cinnarizine ($p = 0.14$) nor fenofibrate ($p = 0.19$) nanoparticles, when compared to the raw compounds. This is in congruence with the conclusion of Murdande et al. (2015), who had not seen any enhancement of solubility upon nanomilling neither when separating the nanoparticles from dissolved drug by ultracentrifugation nor by 0.10 μm nanofiltration (Murdande et al., 2015). Sironi et al. (2017) also measured very similar concentrations of dissolved Fenofibrate over the nanocrystalline marketed product (Lipidil 145) as compared to raw fenofibrate, when separating by 0.10 μm nanofiltration. Interestingly, Imono et al. (2020) measured concentrations of dissolved fenofibrate that were moderately enhanced (up to 1.4-fold) for the nanomilled suspensions, as measured both by fiber-optic UV analysis (using 2nd derivative correction) and upon separation by 0.02 μm filter

Table 2
Equilibrium solubility of fenofibrate and cinnarizine as raw material and nanoparticles after 72 h at 37 °C in phosphate buffer pH 6.5 or in the acceptor media used in the dissolution/permeation experiments; mean $\pm$ SD ($n = 3$).

Particles	Concentration (ng/mL)
Raw fenofibrate	318.21 ± 10.81
Nanomilled Fenofibrate	306.83 ± 3.42
Fenofibrate in 2% SDS	443,982.46 ± 8330.14
Raw cinnarizine	1867.84 ± 18.72
Nanomilled Cinnarizine	1902.05 ± 21.45
Cinnarizine in 5% HP-β-CD	67,669.06 ± 5278.62

by HPLC (Imono et al., 2020).

The unchanged equilibrium solubility above nanoparticles found here as compared to raw drug further corroborates the hypothesis based on solid-state examinations that the nanoparticles are in the same crystal state. At the same time this cannot rule out the transient occurrence of partially amorphous particles. These particles may have recrystallized or undergone particle-changes by Ostwald ripening during the equilibration time of 72 h.

The solubility of fenofibrate and cinnarizine in their respective acceptor media for the permeation experiments were also examined to get an idea if the selected acceptor media provide sink conditions. The apparent solubility was more than 1000-fold higher for fenofibrate in 2% SDS and 35-fold higher for cinnarizine in 5% HP-β-CD. This confirms that absorptive sink conditions in the acceptor compartments were obtained with the chosen acceptor media.

3.4. Dynamic dissolution/permeation experiments

The in vitro performances of nanoparticle suspensions were evaluated using a combined dissolution/permeation set-up in Franz cells and compared to the performances of the raw APIs. The employed setup is limited to passive diffusion of drug and does not account for other properties of the intestinal barrier such as carrier transport, mucus etc. It does, however, allow to gain insight into drug kinetics of permeation and dissolution that is of relevance to understanding the mechanisms that occur during oral drug delivery correlating to differences of particle sizes.

Upon transfer of the cinnarizine raw material into the donor compartment, the concentration increased but did not reach equilibrium solubility within the 4 h of the experiment. Comparing the dissolution profile for raw cinnarizine and its nanoparticles, the dissolution rate for the nanosuspension was persistently higher than for the raw material and approached a higher concentration of dissolved drug approx. by a factor of 1.4 after 4 h (Fig. 4). Especially the initial dissolution process of the nanoparticles was much more rapid, reaching a concentration of approx. 200 ng/mL after 5 min compared to a concentration of the raw particles below LOQ. However, the nanoparticles did not reach equilibrium solubility within the 4 h of the experiment. The dissolution rate of the nanoparticles is significantly higher than the raw API ($p = 0.001$), as expected by the Nernst-Brunner relationship, due to the decreased particle size and increased surface area, possibly also better surface wettability due to nanomilling as cinnarizine crystals are known to have poor wettability (Mishra et al., 2016). The dissolution rate slowed down when approaching higher concentrations for both nanoparticles and raw particles, which is expected from the Noyes-Whitney equation (Noyes and Whitney, 1897), as the bulk concentration approaches solubility. The effect of nanomilling thus can be described as particle size-dependent dissolution rate-enhancement without influence on equilibrium solubility.

The cumulative permeated amount of both the raw cinnarizine and nanoparticles increased with time in a close to linear manner, where the steady-state flux above the nanoparticle suspension was about three times faster than the barrier flux above the raw cinnarizine suspension. This may serve as an indication for the bioavailability-enhancement potential of cinnarizine nanomilling. In fact, Mishra et al. (2016) had reported a 2.5 to 3-fold increase in both C_{max} and plasma AUC upon oral administration of nanomilled cinnarizine as, compared to reference (raw cinnarizine) (Mishra et al., 2016). One should be careful with this correlation, however, because both the preparation method, mean particle sizes and the stabilizers were different in the study by Mishra et al. (2016) as compared to the cinnarizine nanosuspensions investigated here.

For fenofibrate, upon transfer of the raw material into the donor compartment, the concentration increased steadily over the time course of the experiment and reached concentrations of dissolved drug close to the solubility. When the fenofibrate nanosuspension was transferred
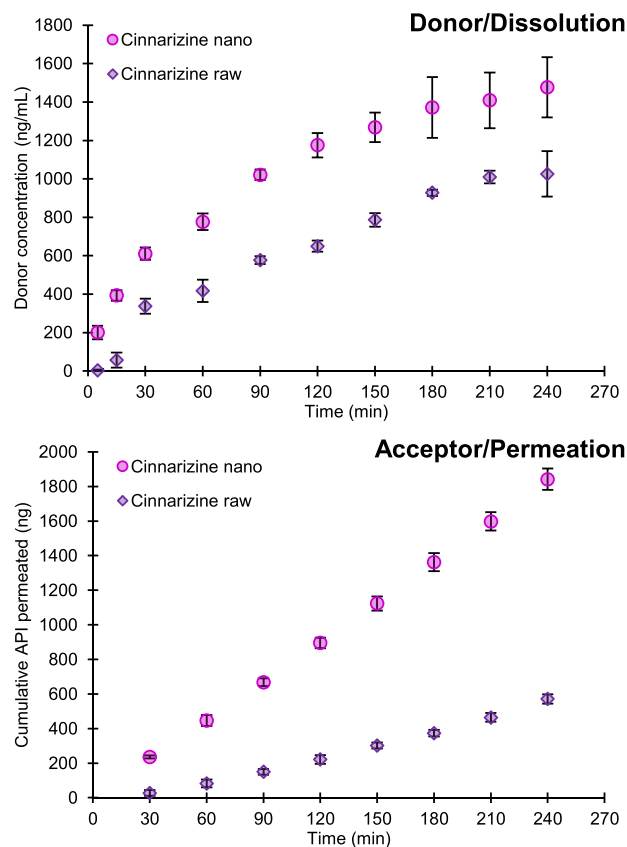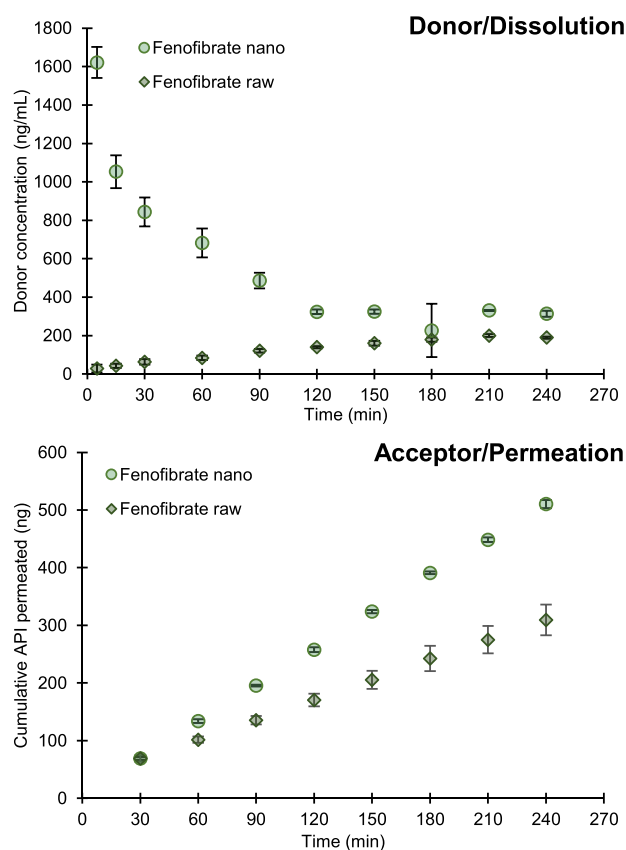

Fig. 4. Dissolution profile depicting the donor concentration as a function of time (top) and permeation expressed as cumulative mass permeated to the acceptor chamber (bottom) for raw cinnarizine (diamonds) and the nanosuspension (circles), reported as mean ± SD ($n = 3$).

into the donor compartment, a significant supersaturation was observed immediately with an initial concentration more than 5-fold higher than equilibrium solubility (Fig. 5). The observed supersaturation was transient with the concentration of dissolved fenofibrate declining to equilibrium solubility during a period of 120 min. The cumulative amount of fenofibrate permeating into the acceptor chamber increased in a close to linear manner over the 4 h of the experiment both for the fenofibrate nanoparticles and the raw particles, where the flux achieved by the nanoparticle suspension was about 2-fold enhanced as compared to that of the raw fenofibrate suspension. A similar dissolution profile with distinct supersaturation had been obtained by Sironi et al. (2017) for Lipidil 145 ONE®, a marketed formulation of fenofibrate nanoparticles containing HPMC and SDS yet tested using a slightly different combined dissolution/permeation setup. This indicates that fenofibrate nanoparticles in the examined formulation composition exhibit a supersaturating nature.

Interestingly, Sironi et al. (2017) demonstrated a beneficial effect of combined dissolution-/permeation as compared to (non-sink) dissolution: the absorptive sink apparently enhanced and prolonged the supersaturation-effect. In yet another study, Imono et al. (2020) demonstrated an excellent correlation between oral bioavailability (initial absorption rate) of nano- and micro-suspensions of fenofibrate of different mean particle sizes and the in vitro flux obtained in a combined dissolution-/permeation experiment using the µFLUX™ setup equipped with a PAMPA barrier. Here, the commercial nanomilled fenofibrate product Tricor® (282 nm) was compared with nanoparticles of 610 nm and 207 nm, produced by rotation/revolution pulverizer at different sets of process conditions (Imono et al., 2020).

The dissolution profiles of cinnarizine and fenofibrate are

Fig. 5. Dissolution profile depicted in the form of the donor concentration as a function of time (top) and permeation expressed as cumulative mass permeated to the acceptor chamber (bottom) of raw fenofibrate (diamonds) and nanosuspension (circles), reported as mean ± SD (n = 3).

substantially different. The fenofibrate nanoparticles supersaturated immediately and precipitated to equilibrium solubility during the experiment. In contrast to this, the dissolution rate of cinnarizine nanoparticles was significantly enhanced when compared to the raw compound (p = 0.001) but did not exhibit any supersaturation. The transient supersaturation followed by precipitation for fenofibrate nanosuspension did not directly translate into decreasing permeation rate, which remained constant (Fig. 5). The reason might be that a considerable fraction of compound in the donor compartment defined as dissolved by filtering through a 0.10 μm filter was not molecularly dissolved but present as distinct nanoparticles below a diameter of 100 nm. Membrane permeation might also be the rate-limiting step for absorption of the fenofibrate nanosuspension in the employed setup as a nearly linear permeation rate is observed, indicating saturated barrier or by limited permeation area. In a recent study, different "dissolved" concentrations were obtained by centrifugation, nanofiltration, and microdialysis, during dissolution, indicating that some apparently dissolved drug is still present even after nanofiltration (Holzem et al., 2022). The measured concentration in the present study using a 5 times larger pore size filter includes possibly a considerable fraction of nanoparticles, in addition to the solubilized drug molecules. Both would not readily permeate, nor are they absorbed in vivo. What is measured as the precipitation of the supersaturated state may thus be the growth of nanoparticles due to the distribution in the medium with no impact on permeation nor absorption. Following the concentration in the donor compartment by alternative methods to catch the molecularly dissolved drug, e.g., by microdialysis as previously described in literature, would be able to study this in more detail and to reveal, whether there is true supersaturation that is worth optimizing the fenofibrate formulation

towards (Fong et al., 2017; Holzem et al., 2022).

Combined dissolution/permeation experiments have been employed to elucidate nanocrystal drug behavior in terms of supersaturation in vitro and at low material use. Dual asymmetric centrifugation is a high throughput method for investigating stabilizer composition and milling process parameters. At this stage of preformulation, it is essential to know whether no supersaturation can be expected, and if the formulation would benefit from increasing the dissolution rate, e.g., by improving the wettability. Or, alternatively, if supersaturation may be expected and it thus could be advantageous to prolong its duration by introducing precipitation inhibitors in the formulations, if this translates into improved permeation rates.

4. Conclusion

In the current study, nanoparticle suspensions of two model drugs have been prepared by a material-sparing dual asymmetric centrifugation method resulting in particle size distributions that are comparable to those obtained with established comminution methods. The poorly soluble compounds fenofibrate and cinnarizine were used as examples. The effects of nanomilling on crystallinity, mean particle diameter and on equilibrium solubility were measured. Finally, the impact of nanonization on in vitro permeability was investigated by in vitro dissolution-permeation studies and compared to in vivo oral pharmacokinetic studies. For both, fenofibrate and cinnarizine, the reduction in particle size down to the minimum of around 300 nm mean diameter had no significant influence on thermodynamic solubility, but significantly enhanced their dissolution rate during combined dissolution/ permeation studies. For none of the two APIs, any indication was seen in XRPD and DSC analysis for changes of the solid state (i.e., bulk crystallinity was retained). Both analytical approaches, however, are generally considered not sensitive enough to detect minute partial disordering on the crystal surfaces.

Although nanosizing led to substantially enhanced dissolution rates for both fenofibrate and cinnarizine, the patterns of the (absorptive sink) dissolution curves differed fundamentally. For the cinnarizine nanosuspension, a shift of the whole dissolution curve towards higher concentrations, but no indication of supersaturation was observed. In contrast, the fenofibrate nanosuspension showed the typical spring & parachute pattern with pronounced supersaturation at early time points, followed by a decline due to precipitation. It is unclear for the time being whether the different (absorptive sink) dissolution behavior, i.e. supersaturation (or not) observed with nanomilled fenofibrate and cinnarizine is a consequence of that fenofibrate more readily forms noncrystalline clusters (partial amorphization) or whether the difference in crystal lattice induces a facilitated release of drug molecules from the highly curved crystal surface or not. The permeation experiments using a combined dissolution/permeation setup, substantiated enhanced permeation rates as compared to the respective raw compounds. For cinnarizine nanoparticles, the permeation rate was found tripled, which is in line with the order of magnitude for in vivo bioavailability enhancement reported earlier in literature. The difference in dissolution/permeation properties between the compounds has direct implication for an informed selection of formulation strategies, may it be the goal to induce and prolong true supersaturation or just to increase the dissolution rate.

A comparison with published in vivo data indicates that it is fair to assume that the enhancement in the permeability rate is the key determinant for oral absorption enhancement of nanocrystal formulations. Furthermore, our findings indicate that in vitro dissolution/permeation studies can be employed to better understand oral absorption enhancement of nanocrystal formulations.

CRediT authorship contribution statement

Jakob Tobias Lynnerup: Conceptualization, Methodology,

Data availability

Data will be made available on request.

Supplementary materials

Supplementary material associated with this article can be found, in the online version, at doi:10.1016/j.ejps.2023.106417.

References

Bauer-Brandl, A., Brandl, M., 2020. Solubility and supersaturation. In: Saal, C., Nair, A. (Eds.), Solubility in Pharmaceutical Chemistry. De Gruyter, pp. 27–70. https://doi.org/10.1515/9783110559835-002.

Bergstrom, C.A.S., Charman, W.N., Porter, C.J.H., 2016. Computational prediction of formulation strategies for beyond-rule-of-5 compounds. Adv. Drug. Deliv. Rev. 101, 6–21. https://doi.org/10.1016/j.addr.2016.02.005.

Bevernage, J., Brouwers, J., Annaert, P., Augustijns, P., 2012. Drug precipitation–permeation interplay: supersaturation in an absorptive environment. Eur. J. Pharm. Biopharm. 82 (2), 424–428. https://doi.org/10.1016/j.ejpb.2012.07.009.

Bitterlich, A., Laabs, C., Busmann, E., Grandeury, A., Juhnke, M., Bunjes, H., Kwade, A., 2014. Challenges in Nanogrinding of Active Pharmaceutical Ingredients [https://doi.org/10.1002/ceat.201300697]. Chem. Eng. Technol. 37 (5), 840–846. https://doi.org/10.1002/ceat.201300697.

Buckley, S.T., Frank, K.J., Fricker, G., Brandl, M., 2013. Biopharmaceutical classification of poorly soluble drugs with respect to "enabling formulations. Eur. J. Pharm. Sci. 50 (1), 8–16. https://doi.org/10.1016/j.ejps.2013.04.002.

Colombo, I., Grassi, G., Grassi, M., 2009. Drug mechanochemical activation [https://doi.org/10.1002/jps.21733]. J. Pharm. Sci. 98 (11), 3961–3986. https://doi.org/10.1002/jps.21733.

Deng, Z., Xu, S., Li, S., 2008. Understanding a relaxation behavior in a nanoparticle suspension for drug delivery applications. Int. J. Pharm. 351 (1–2), 236–243. https://doi.org/10.1016/j.ijpharm.2007.10.001.

Fong, S.Y.K., Poulsen, J., Brandl, M., Bauer-Brandl, A., 2017. A novel microdialysis-dissolution/permeation system for testing oral dosage forms: a proof-of-concept study. Eur. J. Pharm. Sci. 96, 154–163. https://doi.org/10.1016/j.ejps.2016.09.018.

Ghosh, I., Schenck, D., Bose, S., Ruegger, C., 2012. Optimization of formulation and process parameters for the production of nanosuspension by wet media milling technique: effect of Vitamin E TPGS and nanocrystal particle size on oral absorption. Eur. J. Pharm. Sci. 47 (4), 718–728. https://doi.org/10.1016/j.ejps.2012.08.011.

Hagedorn, M., Bögershausen, A., Rischer, M., Schubert, R., Massing, U., 2017. Dual centrifugation – A new technique for nanomilling of poorly soluble drugs and formulation screening by an DoE-approach. Int. J. Pharm. 530 (1), 79–88. https://doi.org/10.1016/j.ijpharm.2017.07.047.

Hagedorn, M., Liebich, L., Bogershausen, A., Massing, U., Hoffmann, S., Mende, S., Rischer, M., 2019. Rapid development of API nano-formulations from screening to production combining dual centrifugation and wet agitator bead milling. Int. J. Pharm. 565, 187–198. https://doi.org/10.1016/j.ijpharm.2019.04.082.

Holsæter, A.M., Wizgird, K., Karlsen, I., Hemmingsen, J.F., Brandl, M., Škalko-Basnet, N., 2022. How docetaxel entrapment, vesicle size, zeta potential and stability change with liposome composition–A formulation screening study. Eur. J. Pharm. Sci. 177, 106267 https://doi.org/10.1016/j.ejps.2022.106267.

Holzem, F.L., Schaffland, J.P., Brandl, M., Bauer-Brandl, A., Stillhart, C., 2022. Microdialysis and nanofiltration allow to distinguish molecularly dissolved from colloid-associated drug concentrations during biomimetic dissolution testing of supersaturating formulations. Eur. J. Pharm. Sci. 174, 106166 https://doi.org/10.1016/j.ejps.2022.106166.

Imono, M., Uchiyama, H., Yoshida, S., Miyazaki, S., Tamura, N., Tsutsumimoto, H., Kadota, K., Tozuka, Y., 2020. The elucidation of key factors for oral absorption enhancement of nanocrystal formulations: in vitro–in vivo correlation of nanocrystals. Eur. J. Pharm. Biopharm. 146, 84–92. https://doi.org/10.1016/j.ejpb.2019.12.002.

Ingebrigtsen, S.G., Didriksen, A., Johannessen, M., Škalko-Basnet, N., Holsæter, A.M., 2017a. Old drug, new wrapping – A possible comeback for chloramphenicol? Int. J. Pharm. 526 (1), 538–546. https://doi.org/10.1016/j.ijpharm.2017.05.025.

Ingebrigtsen, S.G., Škalko-Basnet, N., de Albuquerque Cavalcanti Jacobsen, C., Holsæter, A.M, 2017b. Successful co-encapsulation of benzoyl peroxide and chloramphenicol in liposomes by a novel manufacturing method - dual asymmetric centrifugation. Eur. J. Pharm. Sci. 97, 192–199. https://doi.org/10.1016/j.ejps.2016.11.017.

Juenemann, D., Jantratid, E., Wagner, C., Reppas, C., Vertzoni, M., Dressman, J.B., 2011. Biorelevant in vitro dissolution testing of products containing micronized or nanosized fenofibrate with a view to predicting plasma profiles. Eur. J. Pharm. Biopharm. 77 (2), 257–264. https://doi.org/10.1016/j.ejpb.2010.10.012.

Kataoka, M., Masaoka, Y., Yamazaki, Y., Sakane, T., Sezaki, H., Yamashita, S., 2003. In Vitro System to Evaluate Oral Absorption of Poorly Water-Soluble Drugs: simultaneous Analysis on Dissolution and Permeation of Drugs. Pharm. Res. 20 (10), 1674–1680. https://doi.org/10.1023/A:1026107906191.

Keseru, G.M., Makara, G.M., 2009. The influence of lead discovery strategies on the properties of drug candidates. Nat Rev Drug Discov 8 (3), 203–212. https://doi.org/10.1038/nrd2796.

Kesisoglou, F., Panmai, S., Wu, Y., 2007. Nanosizing — Oral formulation development and biopharmaceutical evaluation. Adv. Drug Deliv. Rev. 59 (7), 631–644. https://doi.org/10.1016/j.addr.2007.05.003.

Knieke, C., Azad, M.A., Davé, R.N., Bilgili, E., 2013. A study of the physical stability of wet media-milled fenofibrate suspensions using dynamic equilibrium curves. Chem. Eng. Res. Des. 91 (7), 1245–1258. https://doi.org/10.1016/j.cherd.2013.02.008.

Kumar, S., Burgess, D.J., 2014. Wet milling induced physical and chemical instabilities of naproxen nano-crystalline suspensions. Int. J. Pharm. 466 (1), 223–232. https://doi.org/10.1016/j.ijpharm.2014.03.021.

Massing, U., Cicko, S., Ziroli, V., 2008. Dual asymmetric centrifugation (DAC)—A new technique for liposome preparation. J. Controlled Release 125 (1), 16–24. https://doi.org/10.1016/j.jconrel.2007.09.010.

Massing, U., Ingebrigtsen, S.G., Škalko-Basnet, N., Holsæter, A.M., 2017. Dual Centrifugation - A Novel "in-vial" Liposome Processing Technique. In: Angel, C. (Ed.), Liposomes. IntechOpen, p. 1. https://doi.org/10.5772/intechopen.68523 pp. Ch.

Mishra, B., Sahoo, J., Dixit, P.K., 2016. Enhanced bioavailability of cinnarizine nanosuspensions by particle size engineering: optimization and physicochemical investigations. Mater. Sci. Eng.: C 63, 62–69. https://doi.org/10.1016/j.msec.2016.02.046.

Murdande, S.B., Shah, D.A., Dave, R.H., 2015. Impact of Nanosizing on Solubility and Dissolution Rate of Poorly Soluble Pharmaceuticals [https://doi.org/10.1002/jps.24426]. J. Pharm. Sci. 104 (6), 2094–2102. https://doi.org/10.1002/jps.24426.

Nernst, W., 1904. Theorie der Reaktionsgeschwindigkeit in heterogenen Systemen. Zeitschrift für Physikalische Chemie 47U (1), 52–55. https://doi.org/10.1515/zpch-1904-4704.

Noyes, A.A., Whitney, W.R., 1897. The rate of solution of solid substances in their own solutions. J. Am. Chem. Soc. 19 (12), 930–934. https://doi.org/10.1021/ja02086a003.

Schmidt, C., Bodmeier, R., 1999. Incorporation of polymeric nanoparticles into solid dosage forms. J. Controlled Release 57 (2), 115–125. https://doi.org/10.1016/S0168-3659(98)00108-4.

Singhal, M., Turunen, E., Ahtola-Sätilä, T., Aspegren, J., Bratty, J.R., Fuhr, R., Ojala, K., van Veen, B., Peltonen, L., 2022. Nanoparticle-based oral formulation can surprise you with inferior in vivo absorption in humans. Eur. J. Pharm. Biopharm. 177, 91–99. https://doi.org/10.1016/j.ejpb.2022.06.009.

Sironi, D., Rosenberg, J., Bauer-Brandl, A., Brandl, M., 2017. Dynamic dissolution-/permeation-testing of nano- and microparticle formulations of fenofibrate. Eur. J. Pharm. Sci. 96, 20–27. https://doi.org/10.1016/j.ejps.2016.09.001.

Tuomela, A., Laaksonen, T., Laru, J., Antikainen, O., Kiesvaara, J., Ilkka, J., Oksala, O., Rönkkö, S., Järvinen, K., Hirvonen, J., Peltonen, L., 2015. Solid formulations by a nanocrystal approach: critical process parameters regarding scale-ability of nanocrystals for tableting applications. Int. J. Pharm. 485 (1), 77–86. https://doi.org/10.1016/j.ijpharm.2015.03.009.

Van Eerdenbrugh, B., Froyen, L., Van Humbeeck, J., Martens, J.A., Augustijns, P., Van den Mooter, G, 2008. Drying of crystalline drug nanosuspensions—The importance of surface hydrophobicity on dissolution behavior upon redispersion. Eur. J. Pharm. Sci. 35 (1), 127–135. https://doi.org/10.1016/j.ejps.2008.06.009.

Van Eerdenbrugh, B., Vermant, J., Martens, J.A., Froyen, L., Van Humbeeck, J., Augustijns, P., Van den Mooter, G, 2009. A screening study of surface stabilization during the production of drug nanocrystals [https://doi.org/10.1002/jps.21563]. J. Pharm. Sci. 98 (6), 2091–2103. https://doi.org/10.1002/jps.21563.

Vinarov, Z., Abrahamsson, B., Artursson, P., Batchelor, H., Berben, P., Bernkop-Schnürch, A., Butler, J., Ceulemans, J., Davies, N., Dupont, D., Flaten, G.E., Fotaki, N., Griffin, B.T., Jannin, V., Keemink, J., Kesisoglou, F., Koziolek, M., Kuentz, M., Mackie, A., Augustijns, P., 2021. Current challenges and future

perspectives in oral absorption research: an opinion of the UNGAP network. Adv. Drug Deliv. Rev. 171, 289–331. https://doi.org/10.1016/j.addr.2021.02.001.

Willmann, A.-.C., Berkenfeld, K., Faber, T., Wachtel, H., Boeck, G., Wagner, K.G., 2022. Itraconazole Nanosuspensions via Dual Centrifugation Media Milling: impact of Formulation and Process Parameters on Particle Size and Solid-State Conversion as Well as Storage Stability. Pharmaceutics 14 (8).

Wang, P., Kui, Q., Miao, Y., Ying, L., He, H., Cai, C., Tang, X., 2012. Improved dissolution rate and bioavailability of fenofibrate pellets prepared by wet-milled-drug layering. Drug Dev. Ind. Pharm. 38 (11), 1344–1353.

Xu, Y., Wang, Y., Huang, Q., Chen, W., Liu, R., Chen, B., Wei, P., 2014. Study of the release of fenofibrate nanosuspension in vitro and its correlation with in situ intestinal and in vivo absorption kinetics in rats. Drug Dev. Ind. Pharm. 40 (7), 972–979.